

Supporting Information

Ultrasensitive 2,4,6-trinitrophenol nanofluidic sensor inspired by olfactory sensory neurons in sniffer dogs

Xin Li,^{af} Zhanfang Liu,^b Linsen Yang,^a Shengyang Zhou,^a Yongchao Qian,^a Yuge Wu,^{af} Zidi Yan,^{af} Zhehua Zhang,^{af} Tingyang Li,^{af} Qingchen Wang,^{af} Congcong Zhu,^{*a} Xiang-Yu Kong,^{acdf} Liping Wen^{*acdef}

^{a.} CAS Key Laboratory of Bio-inspired Materials and Interfacial Science, Technical Institute of Physics and Chemistry, Chinese Academy of Sciences, Beijing 100190, P. R. China.

^{b.} Institute of Forensic Science, Ministry of Public Security, Beijing 100038, P. R. China.

^{c.} Suzhou Institute for Advanced Research, University of Science and Technology of China, Suzhou, Jiangsu 215123, China.

^{d.} School of Chemistry and Materials Science, University of Science and Technology of China, Hefei, Anhui 230026, P. R. China.

^{e.} Qingdao Institute of Bioenergy and Bioprocess Technology, Chinese Academy of Sciences, Qingdao, 266101, P. R. China.

^{f.} School of Future Technology, University of Chinese Academy of Sciences, Beijing 100190, P. R. China.

E-mail: zhucongcong17@mails.ucas.ac.cn;

wen@mail.ipc.ac.cn

Table of Contents

Materials and Methods.....	3
Figure S1. The preparation of AAO@UiO-66-NH ₂	6
Figure S2. The AFM image of unmodified AAO	7
Figure S3. SEM image of the porous side of AAO	8
Figure S4. The quantitative atomic analysis of XPS of AAO@UiO-66-NH ₂	9
Figure S5. The energy-dispersive spectrometer (EDS) of AAO (the porous side)	10
Figure S6. The EDS of AAO (the barrier side).....	11
Figure S7. The EDS of AAO@UiO-66-NH ₂	12
Figure S8. The roughness of AAO and AAO@UiO-66-NH ₂	13
Figure S9. The scheme of combination mechanism between TNP and amino group.....	14
Figure S10. The optical photos of the sample and testing equipment.....	15
Figure S11. The <i>I-V</i> curves of AAO@UiO-66 before and after capturing TNP	16
Figure S12. The XPS of sensors. (a) AAO@UiO-67-NH ₂ and (b) AAO@UiO-68-NH ₂	17
Figure S13. The quantitative atomic analysis of XPS of sensors.....	18
Figure S14. High-resolution X-ray photoelectron spectrum of sensors.....	19
Figure S15. The <i>I-V</i> curves of sensors.....	20
Figure S16. The spatial dimensions of the TNP.....	21
Figure S17. Time stability of AAO@UiO-66-NH ₂	22
Table S1. The global cavity diameter (GLD), pore limiting diameter (PLD) and largest cavity diameter (LCD) of UiO-66-NH ₂ , UiO-67-NH ₂ and UiO-68-NH ₂	23
Supplementary References	24

Materials and Methods

Materials and reagents.

The anodic aluminum oxide (AAO) membranes (with and without barrier layer, pore diameters: 40-70 nm) were purchased from Hefei Pu-Yuan Nano Technology, Ltd., China; Zirconium (IV) chloride ($ZrCl_4$), Benzoic acid, 2-Aminoterephthalic acid (NH_2 -BDC), 2-Amino-[1,1'-biphenyl]-4,4'-dicarboxylic acid (NH_2 -BPDC), 2'-Amino-1,1':4,1''-terphenyl-4,4''-dicarboxylic acid (NH_2 -TPDC), Potassium chloride, (3-Aminopropyl)triethoxysilane (APTES), Ethanol, and N,N-Dimethylformamide (DMF) were purchased from Innochem; all solutions were prepared using Milli-Q water (18.2 M Ω cm).

Preparation of amino-functionalized AAO membrane.

In order to form well-growth metal organic framework layer overhead the AAO, its surface of the barrier layer could be grafted amino-groups. To be more specific, AAO membranes were treated with the ethanol solution of APTES (10% weight) for overnight at 50 °C. Then the AAO was cleaned using ethanol and Milli-Q water successively for three times. At last, amino-functionalized AAO was heated in a vacuum oven for one hour at 110 °C, so that the saline layer will be cross-linked the AAO better.

Fabrication of the AAO@UiO-66-NH₂.

First, $ZrCl_4$ (0.116 g) and benzoic acid (5.06 g) were dissolved in DMF (30 mL), the solution was stirred for 45 min in order to fully dissolve. Then the solution was placed in a Teflon container and heated for 2 h at 80 °C. Then cooling down the container until reaching room temperature. Subsequently, NH_2 -BDC (0.0906 g) was added in the container until completely dissolved. After that, the container was placed into the autoclave, in which the NH_2 -functionalized AAO membranes were placed in a PTFE holder to ensure the AAO could be vertical to the horizontal plane throughout in-situ growth of the UiO-66-NH₂ layer on the AAO process. The autoclave was closed and heated in 120 °C for 48 h^[1]. After the container cooling down to the room temperature, the AAO with UiO-66-NH₂ was placed in DMF for 2 h, then immersed in

ethanol for 12 h. At last, AAO@UiO-66-NH₂ was dried at 50 °C overnight.

Fabrication of the AAO@UiO-67-NH₂.

First, ZrCl₄ (0.3011 g), NH₂-BPDC (0.332 g) and H₂O (0.0232 mol) were dissolved in DMF (25 mL), the solution was stirred for 45 min in order to fully dissolve. After that, the NH₂-functionalized AAO membranes were placed in the container with the PTFE holder. The container was placed in the autoclave and heated in 120 °C for 48 h. After the container cooling down to the room temperature, the AAO with UiO-67-NH₂ was placed in DMF for 2 h, then immersed in ethanol for 12 h. At last, AAO@UiO-67-NH₂ was dried at 50 °C overnight.

Fabrication of the AAO@UiO-68-NH₂.

First, ZrCl₄ (0.24 g), NH₂-TPDC (0.56 g) and H₂O (0.0232 mol) were dissolved in DMF (30 mL). The solution was stirred for 45 min in order to fully dissolve. After that, the NH₂-functionalized AAO membranes were placed in the container with the PTFE holder. The container was placed in the autoclave and heated in 120 °C for 48 h. After the container cooling down to the room temperature, the AAO with UiO-68-NH₂ was placed in DMF for 2 h, then immersed in ethanol for 12 h. At last, AAO@UiO-68-NH₂ was dried at 50 °C overnight.

Characterizations.

Field emission scanning electron microscope (SEM) images were taken from a scanning electron microscopy (Hitachi S-4800, Japan) instrument equipped with an energy dispersive X-ray (EDX) spectrometer under the acceleration voltage of 10 kV. X-ray photoelectron spectroscopy (XPS) spectra were collected on an Al K α source (ESCALAB 250Xi). The zeta potential of AAO@MOFs was measured using a zeta potential analyzer (Anton Paar Surpass 3). The static contact angles of the samples were measured at room temperature using an OCA25 contact angle measuring instrument (Dataphysics, Germany) with an adjustable pick-up lens. X-Ray diffraction (XRD) patterns were collected on a Bruker D8 Focus diffractometer using the incident wavelength of 0.154 nm (Cu K α radiation) and a Lynx-Eye detector. Atomic Force Microscope (AFM) characterization was performed on a Bruker Dimension FastScan Bio. Nitrogen physisorption was conducted at 77 K on a volumetric adsorption

analyzer (Quadrascorb SI-MP, USA).

Electrical Measurement.

The fabricated membrane was mounted between a two-compartment electrochemical cell. The ion transport properties and transmembrane current tests were performed with a Keithley 6487 semiconductor pico ammeter (Keithley Instruments, Cleveland, OH). A pair of homemade Ag/AgCl electrodes were used to apply a transmembrane electrical potential. 0.1 M KCl solution was selected as electrolyte solution. The testing solutions were all prepared using Milli-Q water (18.2 M Ω). Drops of the tested substance were added to the outer surface of the barrier layer of AAO that was functionalized with MOFs. Then rinsed off with deionized water. The platform was placed between two self-made half-cells for electrochemical detection.

Analysis of practical application environment.

The samples in practical environment were prepared from soil in the nearby park and cloth sold commercially. 1 g sample is weighed to add into 10 mL of water. The sample was stirred and immersed in water for ten minutes. Then, the mixed solutions were filtered through polycarbonate porous membrane (the diameter of the pore is 0.1 μm). Finally, the collected solutions were added to the nanofluidic sensor for TNP detection. Particularly, TNP (1 mL of 10^{-13} g/mL) is pre-sprayed on the tested sample for simulating actual environments.

Computational model.

Grand Canonical Monte Carlo (GCMC) simulations with RASPA code were performed to simulate the adsorption behaviors of TNP around the MOF (111) framework. 15 Å vacuum were added to the MOF (111) slab models. The MOFs were considered as rigid in GCMC simulations. The Lennard-Jone parameters of atoms were taken from UFF force field. Ewald method was used to calculate coulombic interactions. All simulations run 106 initialization cycles and 107 production cycles to get data.

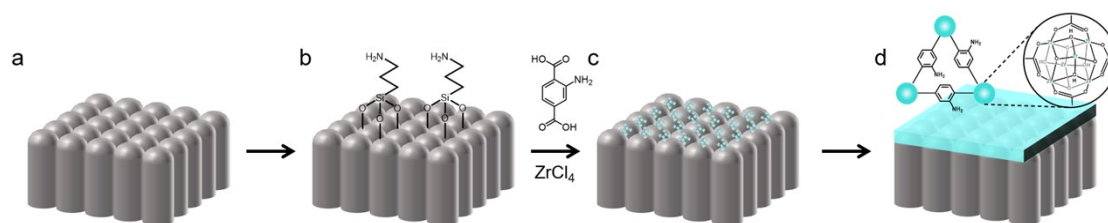


Figure S1. The preparation of AAO@UiO-66-NH₂. (a) The scheme of AAO membrane. (b) NH₂-functionalized AAO is obtained by surface modification of 3-aminopropyltriethoxysilane (APTES). (c) UiO-66-NH₂ is linked to AAO. (d) In situ growth of continuous dense UiO-66-NH₂.

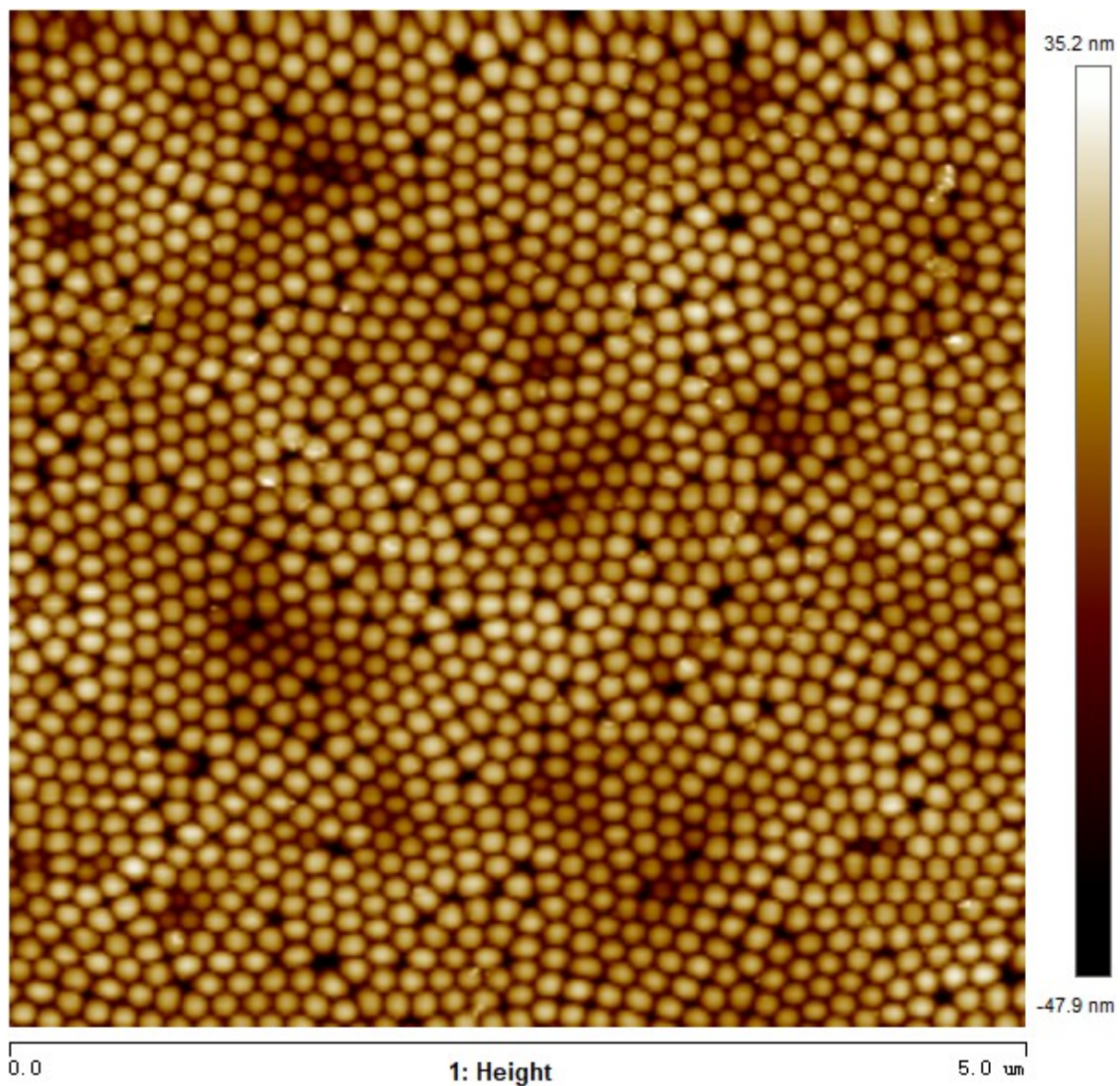


Figure S2. The AFM image of unmodified AAO.

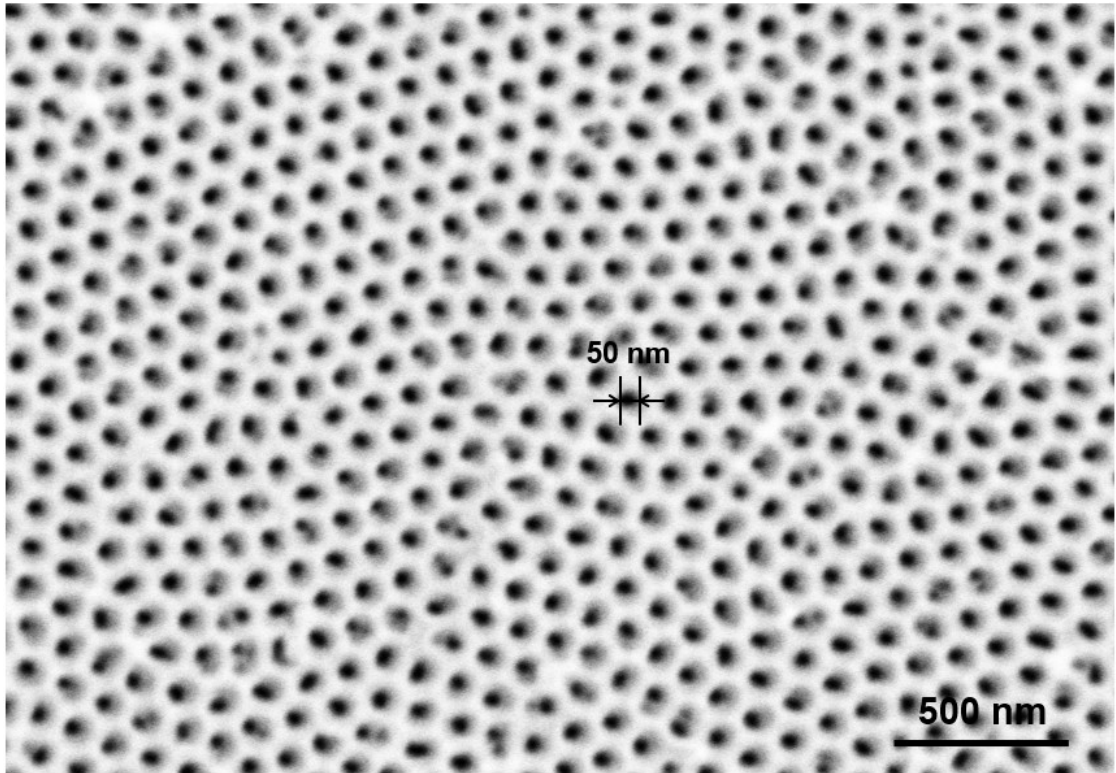


Figure S3. SEM images of the porous side of AAO.

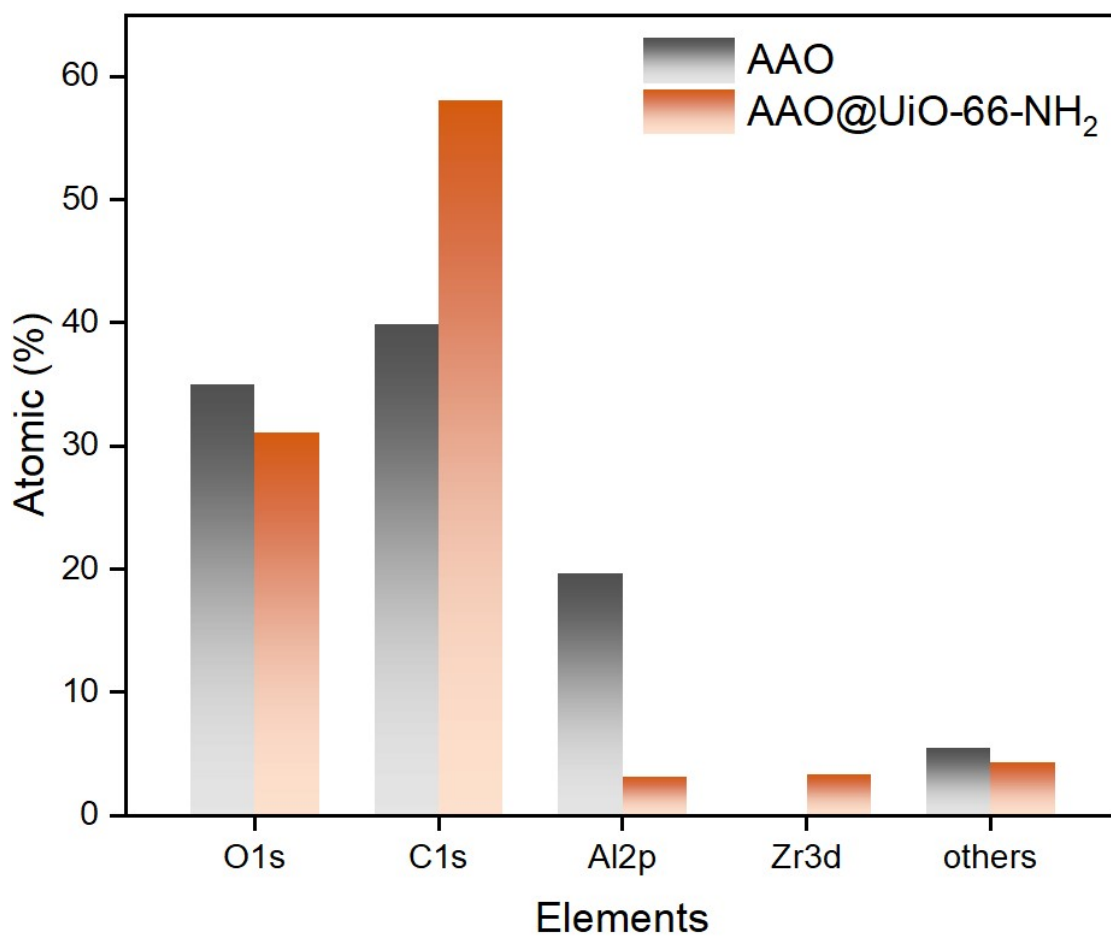


Figure S4. The quantitative atomic analysis of XPS of AAO@UiO-66-NH₂.

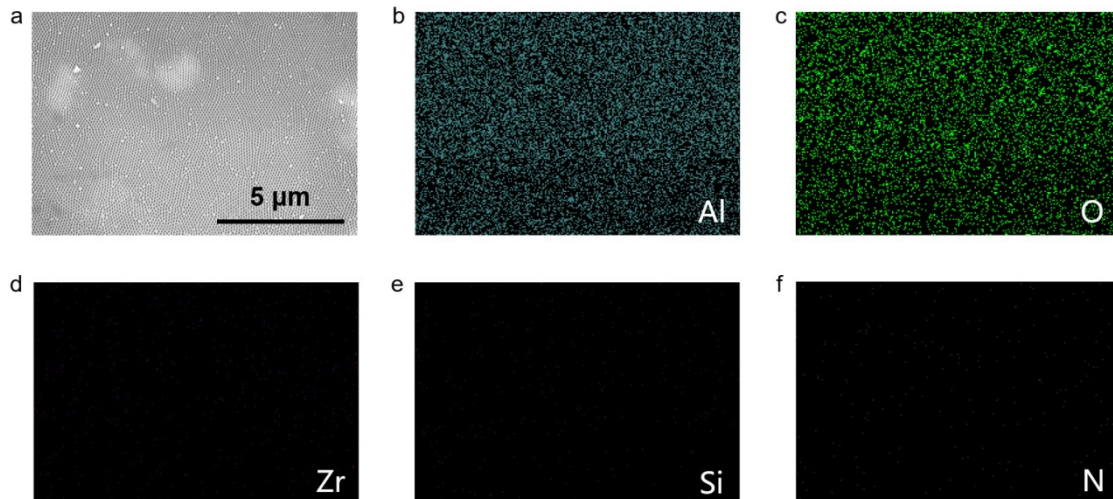


Figure S5. The energy-dispersive spectrometer (EDS) of AAO (the porous side). (a) SEM of the porous side of AAO. (b-f) Elemental mapping of AAO.

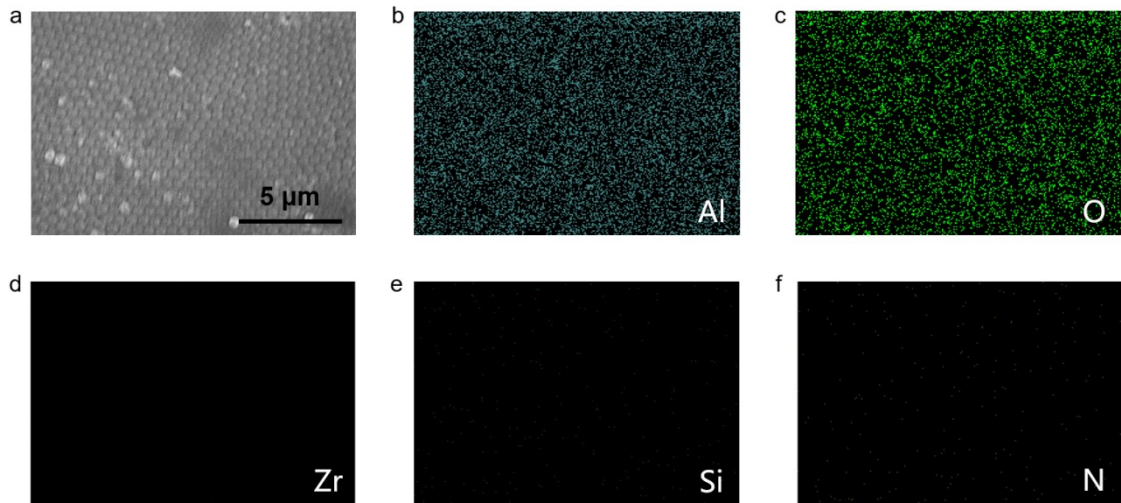


Figure S6. The EDS of AAO (the barrier side). (a) SEM of the barrier side of AAO. (b-f) Elemental mapping of AAO.

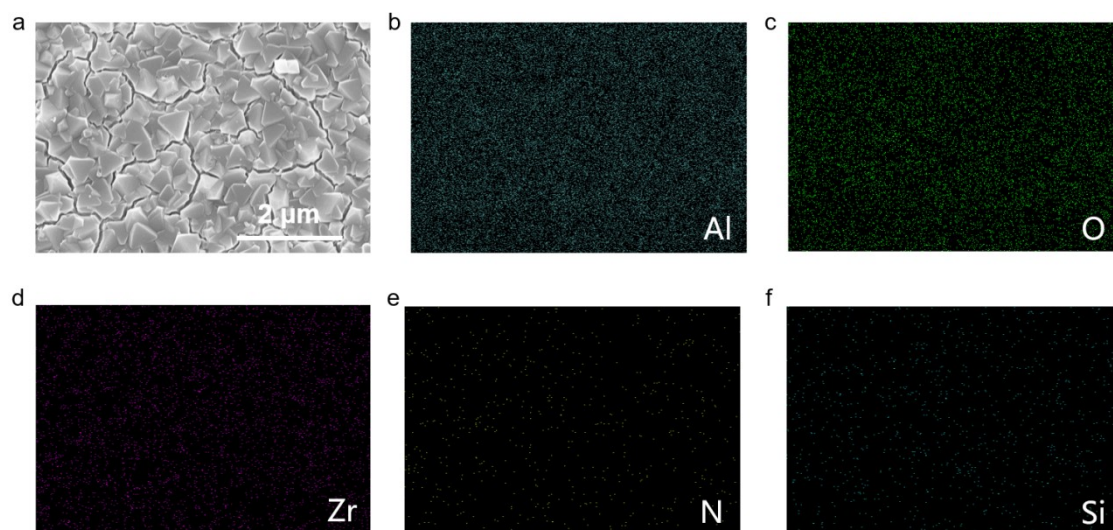


Figure S7. The EDS of AAO@UiO-66-NH₂. (a) SEM of AAO@UiO-66-NH₂. (b-f) Elemental mapping of AAO@UiO-66-NH₂.

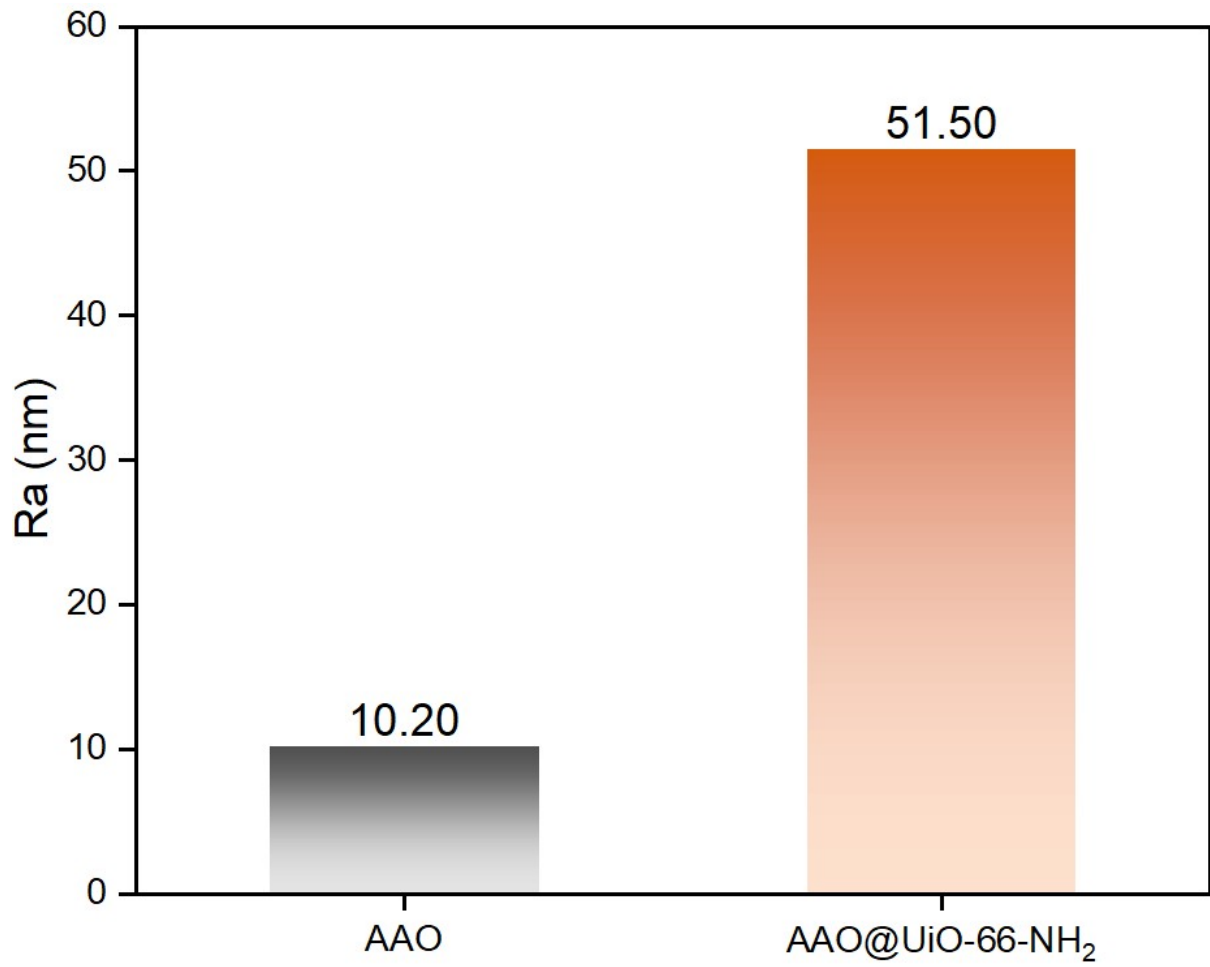


Figure S8. The roughness of AAO and AAO@UiO-66-NH₂.

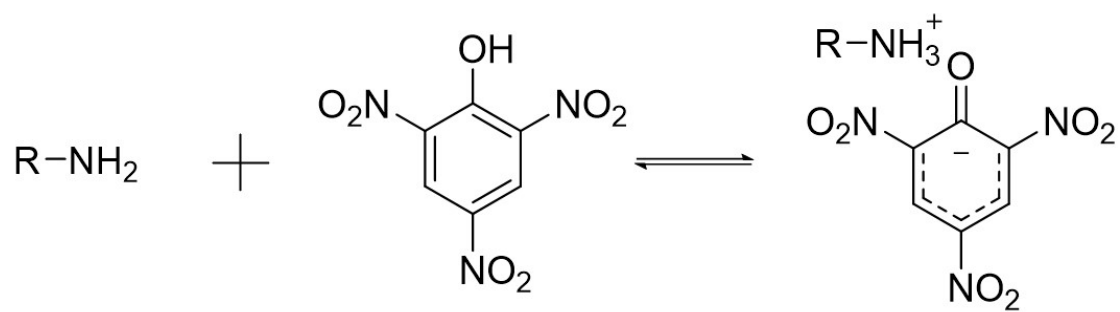


Figure S9. The scheme of combination mechanism between TNP and amino group.

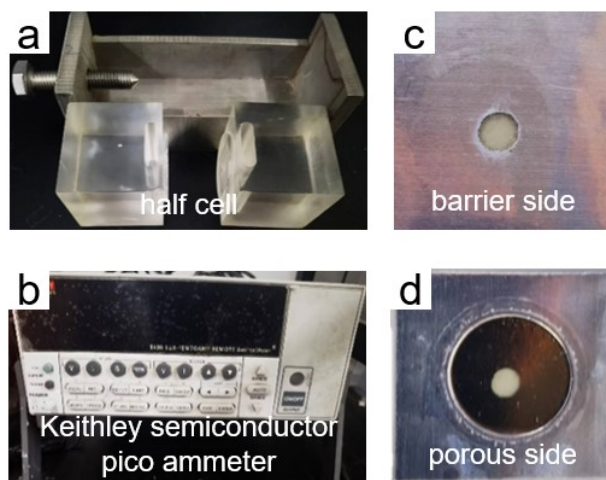


Figure S10. The optical photos of the sample and testing equipment. (a) Two-compartment electrochemical cell. (b) Keithley semiconductor pico ammeter. (c) The barrier side and (d) porous side of the sensing membrane.

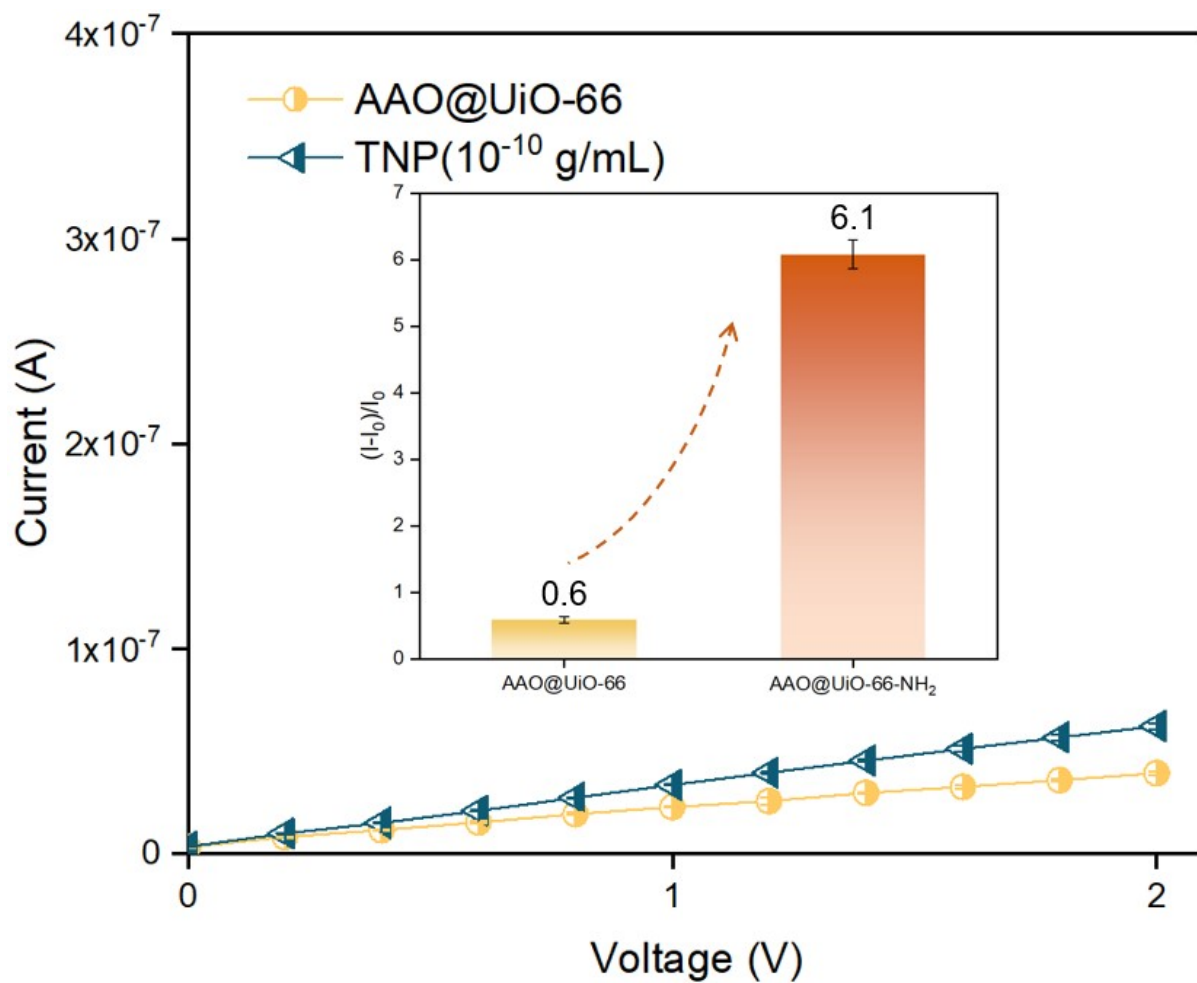


Figure S11. The *I-V* curves of AAO@UiO-66 before and after capturing TNP. Inset: the relative change of currents of AAO@UiO-66 and AAO@UiO-66-NH₂ after capturing TNP.

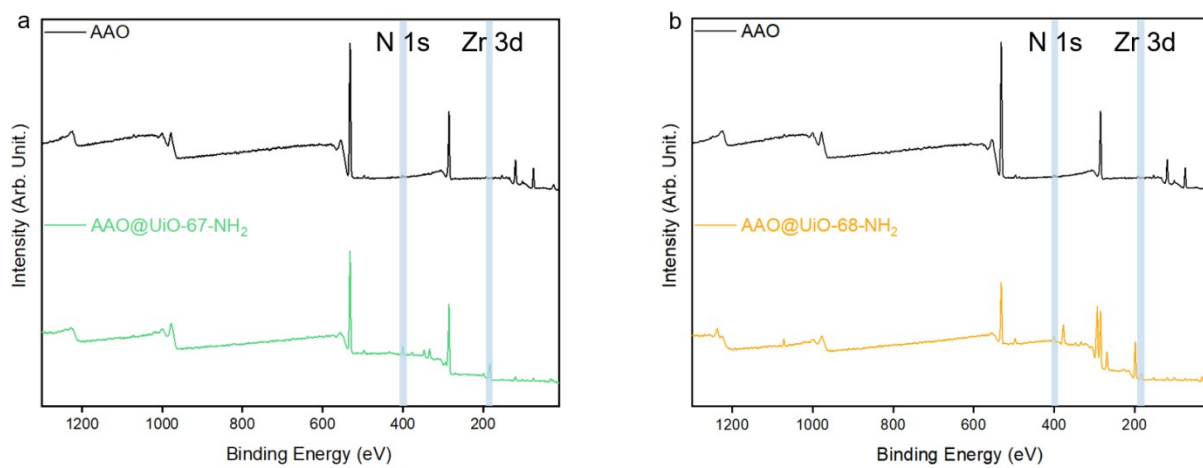


Figure S12. The XPS of sensors. (a) AAO@UiO-67-NH₂ and (b) AAO@UiO-68-NH₂.

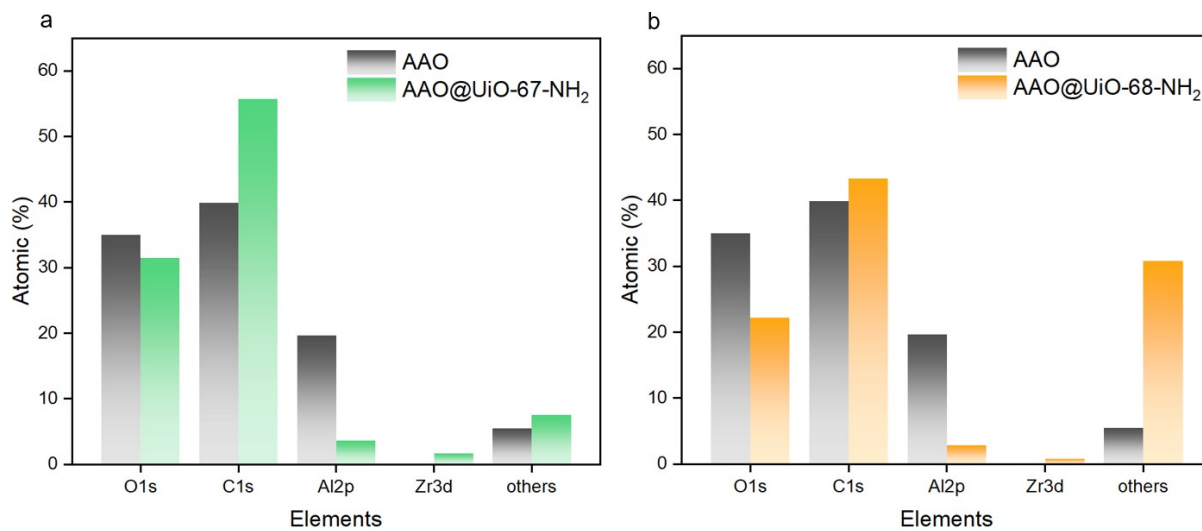


Figure S13. The quantitative atomic analysis of XPS of sensors. (a) AAO@UiO-67-NH₂ and (b) AAO@UiO-68-NH₂.

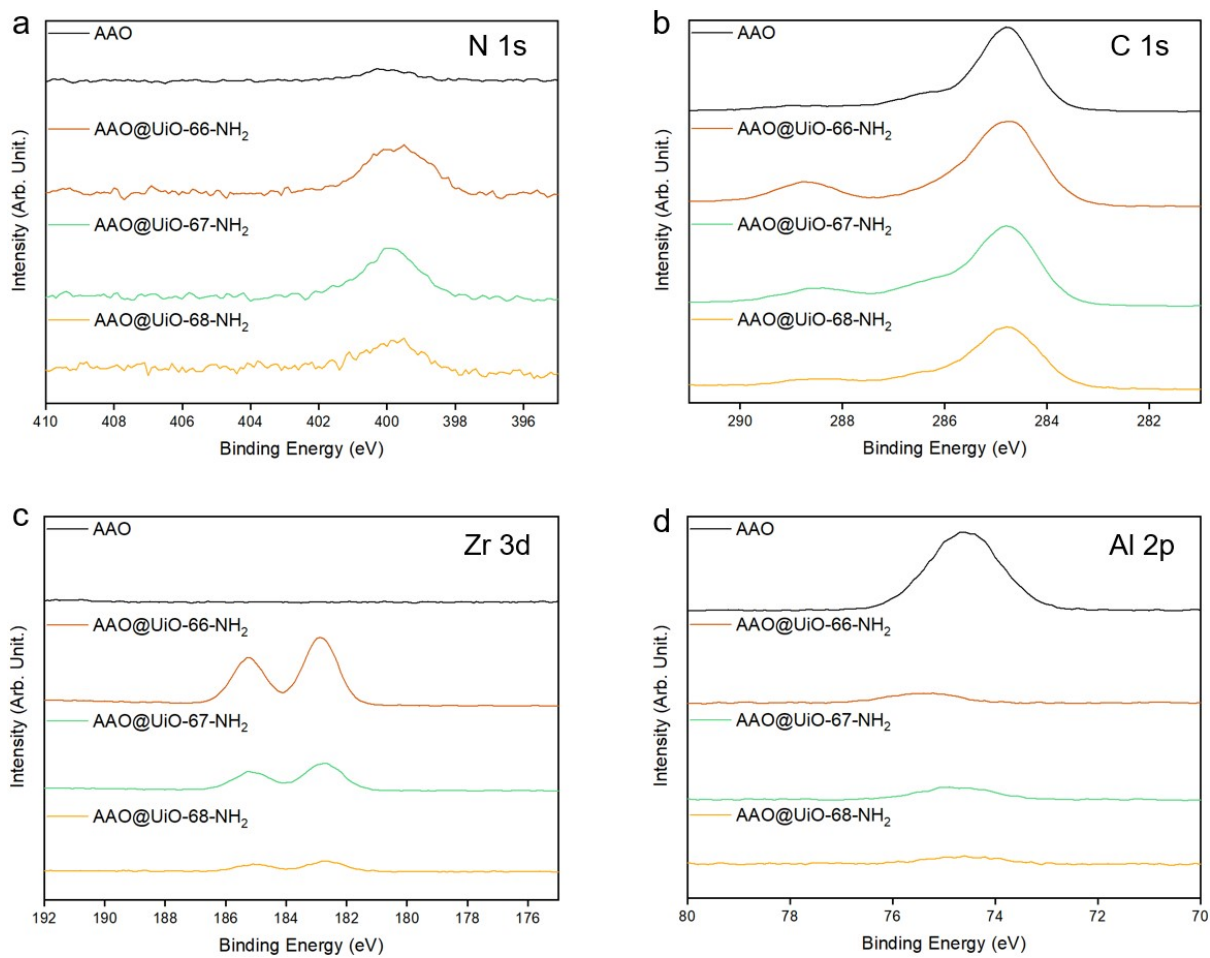


Figure S14. High-resolution X-ray photoelectron spectrum of sensors. XPS of AAO, AAO@UiO-66-NH₂, AAO@UiO-67-NH₂ and AAO@UiO-68-NH₂ in the N 1s (a), C 1s (b), Zr 3d (c) and Al 2p (d) regions.

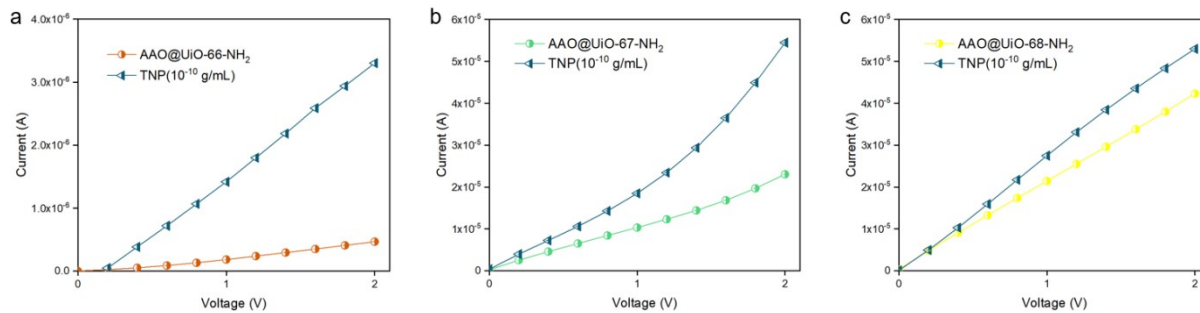


Figure S15. The *I-V* curves of sensors. (a) AAO@UiO-66-NH₂, (b) AAO@UiO-67-NH₂ and (c) AAO@UiO-68-NH₂.

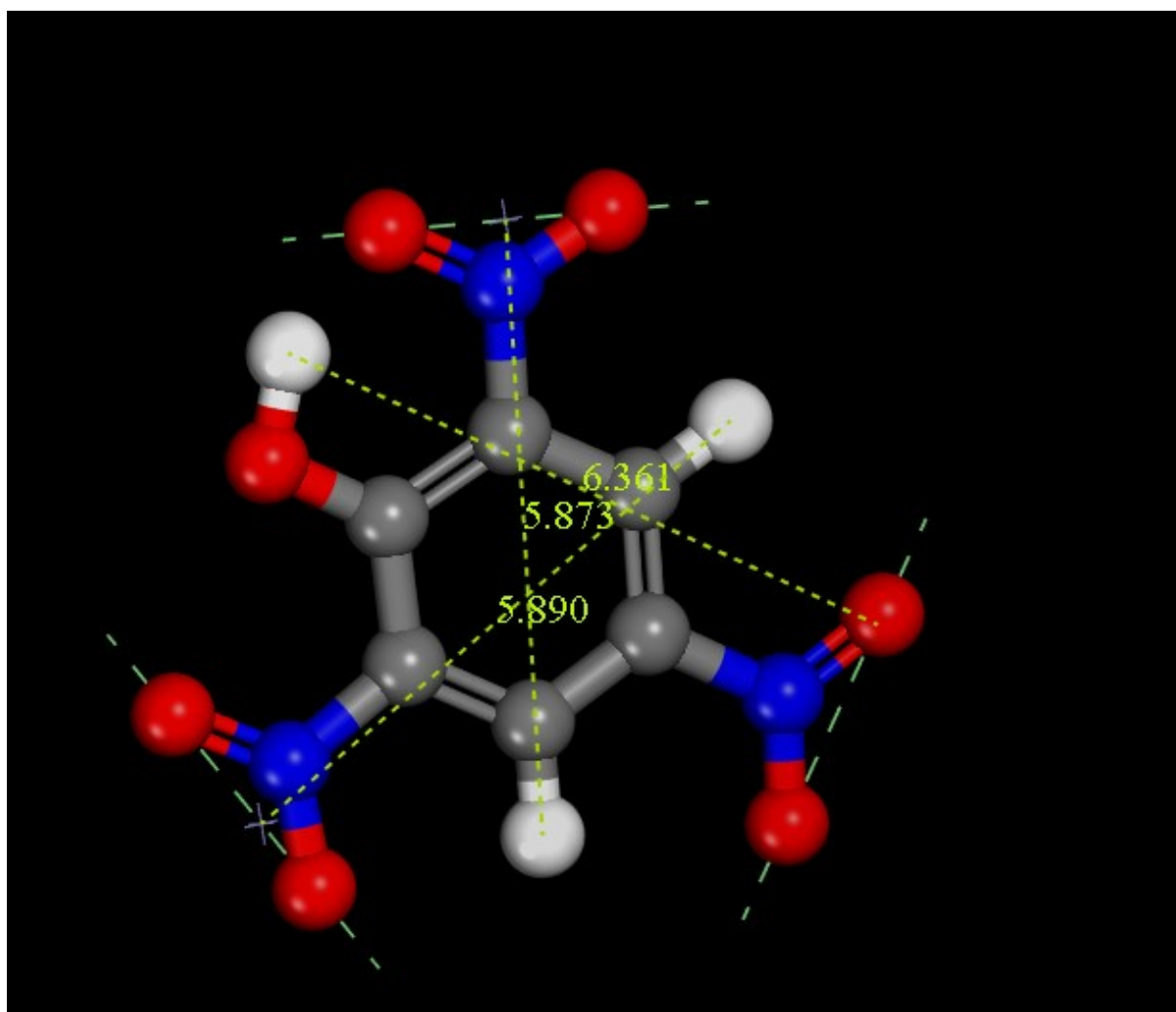


Figure S16. The spatial dimensions of the TNT.

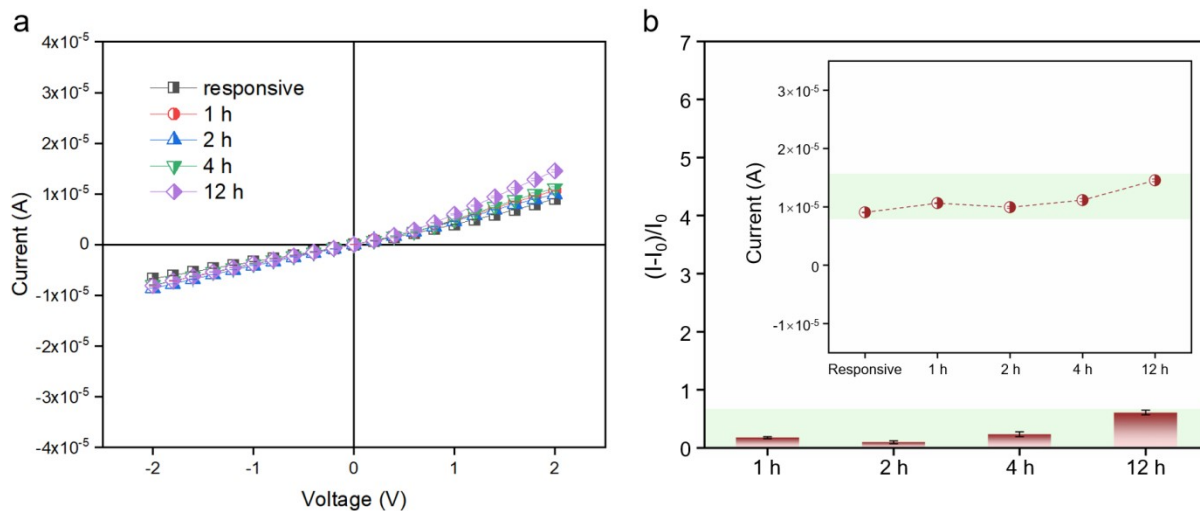


Figure S17. Time stability of AAO@UiO-66-NH₂. (a) *I-V* curves of AAO@UiO-66-NH₂ after placing it at different times. (b) The relative change of currents of AAO@UiO-66-NH₂.

Table S1. The global cavity diameter (GLD), pore limiting diameter (PLD) and largest cavity diameter (LCD) of UiO-66-NH₂, UiO-67-NH₂ and UiO-68-NH₂.

	Global cavity diameter (GLD)	Pore limiting diameter (PLD)	largest cavity diameter (LCD)
UiO-66-NH ₂	7.34791	3.6965	7.34774
UiO-67-NH ₂	11.61957	5.93071	11.6022
UiO-68-NH ₂	15.61494	8.83034	15.29139

Supplementary References

- [1] Y.-C. Liu, L.-H. Yeh, M.-J. Zheng, K. C.-W. Wu, *Sci. Adv.* **2021**, 7, eabe9924.